PHILOSOPHICAL TRANSACTIONS OF THE ROYAL SOCIETY A

*Phil. Trans. R. Soc. A* (2005) **363**, 493–508
doi:10.1098/rsta.2004.1504
*Published online* 13 December 2004

# A 'first principles' potential energy surface for liquid water from VRT spectroscopy of water clusters

By Nir Goldman[1], Claude Leforestier[2] and R. J. Saykally[3]

[1]*Lawrence Livermore National Laboratory, Chemistry and Materials Science Directorate, L-268, Livermore, CA 94551, USA*
[2]*LSDMS (UMR 5636), CC 014, Université Montpellier II, 34095 Montpellier Cédex, France*
[3]*Department of Chemistry, University of California, Berkeley, CA 94720-1416, USA* (saykally@uclink4.berkeley.edu)

We present results of gas phase cluster and liquid water simulations from the recently determined VRT(ASP-W)III water dimer potential energy surface (the third fitting of the Anisotropic Site Potential with Woermer dispersion to vibration–rotation–tunnelling data). VRT(ASP-W)III is shown to not only be a model of high 'spectroscopic' accuracy for the water dimer, but also makes accurate predictions of vibrational ground-state properties for clusters up through the hexamer. Results of ambient liquid water simulations from VRT(ASP-W)III are compared with those from *ab initio* molecular dynamics, other potentials of 'spectroscopic' accuracy and with experiment. The results herein represent the first time to the authors' knowledge that a 'spectroscopic' potential surface is able to correctly model condensed phase properties of water.

**Keywords: liquid water simulation; water clusters; water potential energy surface; first principles water; diffusion quantum Monte Carlo; vibration–rotation–tunnelling spectroscopy**

## 1. Introduction

Literally hundreds of effective potential energy surfaces have now been developed for the purpose of computing properties of liquid water and aqueous solutions via classical (molecular dynamics (MD) or Monte Carlo (MC)) simulations. While the use of these surfaces has engendered much progress in understanding the properties of aqueous systems, there always remains a degree of doubt concerning the validity of simulations results because of the simplistic and empirical nature of these potential surfaces (Guillot 2003). This is particularly the case when properties are computed outside the range of conditions for which the effective surfaces were parametrized (Guillot 2003).

One contribution of 17 to a Discussion Meeting 'Configurational energy landscapes and structural transitions in clusters, fluids and biomolecules'.

These empirical potential surfaces are generally formulated by using classical simulations to adjust a simple analytical expression to structural and thermodynamic properties of bulk water (see Berendsen *et al.* 1987; Jorgensen *et al.* 1983). Accordingly, quantum effects (tunnelling through potential barriers to hydrogen-bond rearrangement, zero-point energies) are not properly represented, and the corresponding intermolecular potential energy surfaces (IPSs) are artificially 'smoothed', relative to the topology of the true quantum surface (i.e. with the actual potential barriers and deeper potential wells). Hence, it is not surprising that quantum simulations employing such classical effective potentials yield the conclusion that quantum effects in ambient liquid water are small, equivalent to simply raising the temperature in a classical simulation by 50 °C (Del Buono *et al.* 1991; Kuharsky & Rossky 1985).

The development of *ab initio* molecular dynamics methods has been a great advance in the study of condensed matter systems, mitigating the above concerns regarding the use of effective potentials. However, these involve the use of fully quantum potentials in classical simulations, and might therefore underestimate those dynamics for which sizeable potential barriers exist in the pathway, e.g. hydrogen-bond rearrangement in liquid water. Moreover, their dependence on density functional theory methods for computing the electronic energy, and the resulting difficulty in determining non-local interactions (dispersion) (Stone 1996), engenders an element of uncertainty in calculations of systems for which such interactions are known to be important (note that dispersion constitutes *ca.* 20% of the cohesive energy of water (Rybak *et al.* 1991)). Finally, concerns have been raised regarding the convergence of *ab initio* MD methods (Grossman *et al.* 2004). These facts make it clear that further study of the water force field is in order.

## 2. Determination of the $(H_2O)_2$ potential surface

In order to address these issues, we have taken a bottom-up 'first principles' approach in which we have created a liquid potential through highly accurate determination of dimer properties. In a recent paper, Hodges *et al.* (1997) calculate the total *ab initio* interaction energies for the water trimer, tetramer and pentamer and dissect them into their respective $N$-body components. The results show that the two-body forces comprise *ca.* 75% of the total energy, the three-body terms *ca.* 20%, and the four-to-five-body terms the remaining 5%. In a more detailed paper, Ojamäe & Hermansson (1994) performed a similar analysis of many-body forces operative in chains of water molecules up to the heptamer, in ring structures up to the pentamer, and in a tetrahedral pentamer. These calculations, performed at the MP2 level, yield some striking insights. In both the water heptamer chain and the pentamer-ring structure, they find that two-body forces account for over 80% of the total interaction energy, and that two- and three-body terms together account for over 99%. In the tetrahedral pentamer, which closely resembles the average liquid and normal ice structures, they find that the two-body energy constitutes over 87% of the total interaction energy, and the two- and three-body terms together comprise *ca.* 99.6%. In all cases, the total energies of larger clusters are rapidly converging and are essentially fully converged by accounting for only the two- and three-body terms. Hence, rigorous description of the pairwise interaction appears to be the central issue for constructing a complete molecular (i.e. non-empirical) description of the liquid.

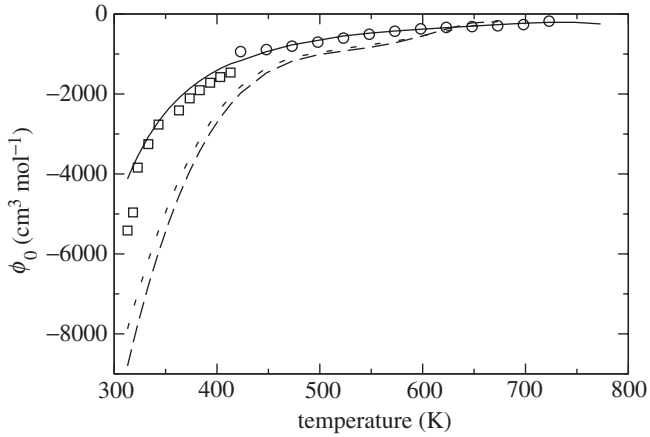


Figure 1. Joule–Thomson coefficient for $(H_2O)_2$ from VRT(ASP-W)III, in comparison with experiment. The solid black line corresponds to VRT(ASP-W)III, the open squares to experimental results from McGlashan & Wormald (2000), the open circles to experimental results from Kell *et al.* (1989), the dotted line to ASP-W (Millot & Stone 1992), and the dashed line to TIP4P (Jorgensen *et al.* 1983). The discrepancies evident at lower temperatures are due to the truncation of quantum effects in the calculated SVC to first order.

A series of new IPSs, formulated by refining *ab initio*-based analytical surfaces against the extensive vibration–rotation–tunnelling (VRT) spectroscopy data now available for the water dimer, has been reported by two groups. One of the most accurate water dimer potentials obtained to date is the recently determined VRT(ASP-W)III water dimer IPS (see Goldman *et al.* 2002 and references therein). This is the third fitting of Millot & Stone's (1992) rigid ASP-W *ab initio* potential to $(D_2O)_2$ VRT transitions. The dimer tunnelling splittings resulting from hydrogen-bond rearrangements and the intermolecular vibrational frequencies provide a highly sensitive probe of the complex water IPS (Saykally & Blake 1993), and such measurements have been made extensively by our laboratory (Braly *et al.* 2000*a*,*b*; Busarow *et al.* 1989). The ASP-W potential has 72 parameters, corresponding to electrostatic interactions, two-body exchange–repulsion, two-body dispersion and many-body induction, but it was found previously that accurate fits to the data could be produced by fitting just a few of the 22 exchange–repulsion parameters (Fellers *et al.* 1999). Thus, the VRT(ASP-W)III potential was generated by fitting six of the exchange–repulsion parameters to 30 far-infrared and microwave transitions. This IPS constitutes a substantial improvement over the original VRT(ASP-W) potential (see Goldman *et al.* 2002 and references therein), although Groenenboom *et al.* (2000) have obtained one of comparable quality for the $(H_2O)_2$ isotopomer by 'tuning' an *ab initio* potential derived from symmetry adapted perturbation theory (SAPT) against VRT spectra.

The VRT(ASP-W)III yields excellent values for the dimer binding energy and structure (table 1), as well as the zero-pressure isothermal Joule–Thomson coefficient, $\phi_0$ (figure 1). The zero-pressure Joule–Thomson coefficient is related to the second virial coefficients (SVCs) via the equation

$$\phi_0 = B - T\frac{\mathrm{d}B}{\mathrm{d}T},$$

where $B$ is the temperature-dependent SVC, $T$ is the temperature, and $\mathrm{d}B/\mathrm{d}T$ is the derivative of $B$ with respect to $T$ (McGlashan & Wormald 2000). Due to the derivative information inherent within the coefficient, it provides a more stringent test of the IPS than the SVCs do themselves. We have recently shown that the quantum corrected SVCs computed from VRT(ASP-W)III also agree nearly perfectly with experimental results over a wide range of temperatures (see Goldman *et al.* 2002 and references therein). Combining the data from McGlashan & Wormald (2000) with the values of $\phi_0$ calculated from the $B(T)$ results from Kell *et al.* (1989) allows us to test the validity of two-body interaction terms from VRT(ASP-W)III over an even wider range of temperatures. The computed values of $\phi_0$ agree very closely with experiment.

## 3. Diffusion quantum Monte Carlo results for $(H_2O)_2$–$(H_2O)_6$

The excellent reproduction of dimer properties over such a wide temperature range establishes that VRT(ASP-W)III is an excellent model of two-body properties of water. Moreover, since it also rigorously represents the leading many-body terms (due to 'polarization' or 'induction') in terms of a tensorial polarizability and multipole moments, VRT(ASP-W)III can also correctly describe the trimer, tetramer and larger water clusters.

Many VRT spectroscopic data exist for larger clusters, particularly ground-state properties of up to hexamer (Liu *et al.* 1994, 1996*a–c*, Liu *et al.* 1997; Pugliano & Saykally 1992). We can thus simulate larger clusters with these potentials and compare results with the VRT data in order to further test the validity of our IPS models. Diffusion Monte Carlo (DMC) simulation is a useful technique for such purposes (Goldman & Saykally 2004; Gregory & Clary 1994, 1995*a*,*b*, 1996*a*,*b*; Gregory *et al.* 1997). It is a fully quantum-mechanical technique with a computational cost that scales favourably with cluster size and potential complexity. Furthermore, it is an excellent complement to *ab initio* calculations because directly observable vibrationally averaged properties, rather than just the (unobservable) equilibrium properties are calculated. Quack, Suhm and co-workers have used DMC extensively in similar studies of $(HF)_n$ clusters (Kloppera *et al.* 1998; Quack & Suhm 1990, 1991*a*,*b*; Quack *et al.* 2001) and have determined highly accurate potentials for HF aggregates.

The details of our calculations and the corresponding results have been summarized elsewhere (Goldman & Saykally 2004). Thus, we only provide a summary of the technique and results below. The starting point of a DMC simulation is the time-dependent Schrödinger equation, which is rewritten in imaginary time and thus becomes isomorphic with the diffusion equation. Consequently, the eigenstate of interest can be simulated via random diffusion. All of the IPSs used in the cluster calculations herein use a 'frozen monomer' approximation, in which intramolecular degrees of freedom are not explicitly included in the calculation. Such IPSs will be henceforth referred to as rigid potentials. Since intermolecular degrees of freedom are treated separately from intramolecular vibrations, and are of a lower frequency, a larger time-step can be used in the rigid-body simulations. A simple method for treating monomers as rigid bodies, called the rigid-body discrete Monte Carlo (RBDMC), has been developed by Buch and co-workers (Buch 1992; Sandler *et al.* 1994) and again the reader is referred to the those references for further information.

Table 1. *Water dimer equilibrium and vibrational ground-state properties from VRT(ASP-W)III, with comparison with experiment (Keutsch & Saykally 2001)*

(Using these data in conjunction with measurements for other dimer isotopes, Keutsch & Saykally derived the equilibrium structure parameter, $R_{OO}$. The experimental observables, $A$, $(B + C)/2$ and $B - C$ are taken from Braly (1999, pp. 130, 170). As stated in the text, the VRT(ASP-W)III vibrationally averaged properties were determined by DMC. The rotational constants were calculated using fixed monomer geometries of $R_{OH} = 0.9572$ Å and $\angle$HOH $= 104.52°$, and masses $H = 1.007\,0511$ and $O = 15.994\,915$ atomic units. The equilibrium properties from VRT(ASP-W)III, listed above, were calculated by the ORIENT molecular-interaction program, from Stone *et al.* (2000).)

| | experiment | VRT(ASP-W)III$_{vib}$ | VRT(ASP-W)III$_{eq}$ |
|---|---|---|---|
| $D_e$ (kcal mol$^{-1}$) | 5.40 (0.5) | — | 4.96 |
| $D_0$ (kcal mol$^{-1}$) | 3.66 (0.5) | 3.09 | — |
| $R_{OO}$ (Å) | 2.976 (0.00, −0.03) | 3.01 | 2.95 |
| $A$ (GHz) | 227.6 | 230.36 | 220.06 |
| $(B + C)/2$ (GHz) | 6.16 | 5.96 | 6.24 |
| $B - C$ (MHz) | 33.11 | 70 | — |

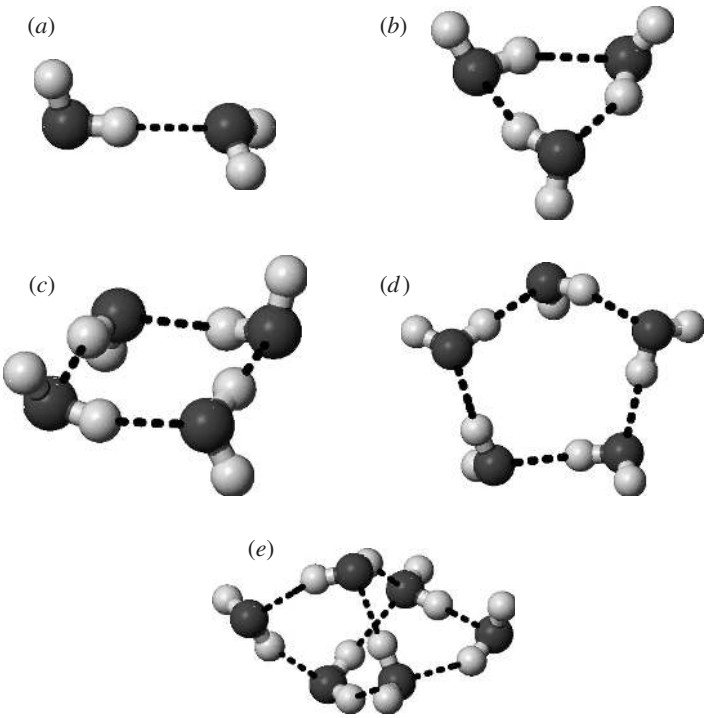


Figure 2. Vibrational ground-state structures from VRT(ASP-W)III: (*a*) dimer; (*b*) trimer (uud); (*c*) tetramer (udud); (*d*) cyclic; (*e*) cage.

Computed equilibrium properties of the trimer through hexamer agree very well with the best available *ab initio* results (table 2), and vibrationally averaged ground state structures for all structures computed with DMC simulations agree well with

Table 2. *Comparison of minimum energy structures to best available ab initio results (Burnham & Xantheas 2002b)*

(Equilibrium structures from VRT(ASP-W)III were calculated by the ORIENT program (Stone *et al.* 2000). Results from VRT(ASP-W)III are very close to the *ab initio* energetic ordering of results (Goldman & Saykally 2004). More importantly, the IPS predicts the correct energetic ordering of the hexamer prism and cage structures. This ordering is reversed when quantum zero-point energies are taken into account (Goldman & Saykally 2004).)

| | VRT(ASP-W)III | *ab initio* |
|---|---|---|
| $(H_2O)_2$ | −4.96 | −4.98 |
| $(H_2O)_3$ | −15.53 | −15.8 |
| $(H_2O)_4$ | −28.74 | −27.6 |
| $(H_2O)_5$ | −38.31 | −36.3 |
| $(H_2O)_6$ cage | −48.80 | −45.8 |
| $(H_2O)_6$ prism | −49.97 | −45.9 |

Table 3. *Rotational constants from VRT(ASP-W)III for the water trimer through hexamer, in comparison with experiment*

('AF' denotes that the $C$ rotational constant could not be measured for a given cluster, and thus its value was 'arbitrarily fixed'. $H_2O$ results are not available for the tetramer and pentamer, so $D_2O$ results are presented instead.)

| | $(H_2O)_3$ | | $(D_2O)_4$ | | $(D_2O)_5$ | | $(H_2O)_6$ | |
|---|---|---|---|---|---|---|---|---|
| | VRT | expt | VRT | expt | VRT | expt | VRT | expt |
| $A$ (GHz) | 6.84 | 6.65 | 3.18 | 3.08 | 1.83 | 1.75 | 2.14 | 2.16 |
| $B$ (GHz) | 5.68 | 6.65 | 2.77 | 3.08 | 1.60 | 1.75 | 1.07 | 1.13 |
| $C$ (GHz) | 3.15 | 3.51 (AF) | 1.54 | (AF) | 0.85 | (AF) | 1.04 | 1.07 |

experimental data (tables 1 and 3, figure 2). As shown, VRT(ASP-W)III performs very well as a model for higher-order clusters. Upon examination of results for the pentamer and hexamer, it is clear that it represents a substantial improvement over previous fittings (Goldman & Saykally 2004). Notably, the DMC calculation on VRT(ASP-W)III correctly predicts that the cage form of the hexamer is the most stable of several low-energy structural isomers, as established by terahertz experiments (Keutsch & Saykally 2001). As we have noted, this is surprising, considering that VRT(ASP-W)III represents a relatively minor refinement of the previous version in terms of dimer properties. However, this subtle refinement has major global consequences, since VRT(ASP-W)III is a much better model for the larger clusters. Hence, continued fitting of ASP-W or other IPS to larger spectroscopic datasets seems to be a worthwhile pursuit.

The fact that the only many-body force present in VRT(ASP-W)III is induction supports the assertion that for gas-phase cluster calculations it seems reasonable to neglect all other many-body contributions (i.e. dispersion, exchange); hence, the computational cost of including three-body exchange in VRT(ASP-W)III does not seem worthwhile. Given the above encouraging results, we performed classical MC simulations of ambient liquid water to determine how well the dimer-based IPS would

perform, recognizing that while the dominant many-body interaction (induction) was well-represented by the ASP-W versions, the much smaller three-body exchange terms were omitted.

## 4. Liquid water simulations

Here we employ our VRT(ASP-W)III water dimer potential in MC simulations of bulk liquid water, in order to explore and characterize the nature of the subtle many-body effects that must be added to this polarizable dimer potential in order for it to properly describe bulk properties. We note that because VRT(ASP-W)III contains a tensorial polarizability, it will accurately represent the leading many-body interaction, namely induction, since the remaining important many-body terms (namely three-body exchange, three-body dispersion) are much smaller.

In the sections below, the results for the radial distribution functions from VRT(ASP-W)III are discussed, and comparison is made with experiments (Hura *et al.* 2000; Soper 2000). The MC simulation technique will not be reviewed, and the reader is directed to Allen & Tildesley (1989) and Frenkel & Smit (1996) for further information. Comparison is also made with results from Car–Parrinello molecular dynamics (CPMD), since this represents a different yet equally valid approach to developing a 'first principles' model for liquid water. Also noteworthy is the TTM2-R potential, developed by Burnham and Xantheas (Burnham & Xantheas 2002*a–c*; Xantheas *et al.* 2002), which accurately models equilibrium properties (i.e. without quantum zero-point effects taken into account) of water clusters as well as structural properties of liquid water and ice. However, TTM2-R reportedly does not accurately reproduce the water dimer VRT spectrum (Mas *et al.* 2003*b*). Hence, given our ultimate goal of developing a 'perfect dimer potential' in order to ascertain the nature of the many-body forces acting within the liquid, results from TTM2-R are not included in the present study.

### (*a*) *VRT(ASP-W)III*

#### (i) *Monte Carlo simulations*

In order to simulate liquid water properties with VRT(ASP-W)III, we used MC rather than MD because MC has the advantage of transcending calculations of intermolecular forces, as well as the concomitant disadvantage of not yielding dynamical information. Given the complexity of the IPS, namely 72 parameters and iterated induction, calculation of the intermolecular forces would be prohibitively expensive. Unless indicated otherwise, our simulations were conducted in the canonical (NVT) ensemble with 64 monomers in a cubic box at ambient density of $1.0\ \mathrm{g\ cm^{-3}}$ and a temperature of 25 °C. The simulation was started from an equilibrated MD simulation with the MCY potential (Matsuoka *et al.* 1976). The minimum image convention was applied when calculating distances between centre of masses of molecules, and when long-range interactions were neglected, interactions were truncated within a cut-off radius equal to half the box length. In order to test the suitability of this cut-off radius, simulations were run at the above density and temperature for systems comprising 32–108 monomers, and the $g(R_{\mathrm{OO}})$ radial distribution functions (RDFs) were already converged at a simulation size of 64 monomers. To ensure accurate structural determination from the IPS and adequate simulation times, the

results from VRT(ASP-W)III presented below are from simulations of 64 monomers, performed with truncation of the long-range forces.

These were run for *ca.* 5000 cycles, where one cycle is equal to $N$ Monte Carlo moves, where $N$ is equal to the number of molecules in the simulation. The minimum image convention was applied when calculating distances between centre of masses of molecules. In general, long-range electrostatic interactions in liquid simulations can be handled via Ewald sums, the details of which can be found in Allen & Tildesley (1989); Frenkel & Smit (1996), but because ASP-W contains up to a quadrupole on the oxygen and dipoles on the hydrogens, full Ewald sums were too costly to use in these simulations. Simulations of 32 monomers were run with the charge–charge Ewald sums, only, in order to test their importance, and preliminary results indicated that the Ewald sums had little effect on the RDFs computed from VRT(ASP-W)III. Thus, the residual electrostatics were truncated at a cut-off of half the box length. Maximum atomic translational moves of 0.4 Å yielded acceptance ratios of roughly 60%, and molecules were kept rigid via the SHAKE algorithm (Ryckaert *et al.* 1977). Simulations performed with VRT(ASP-W)III had induction and dispersion damped with the same hardness factors as for our gas phase calculations (see Goldman *et al.* 2002 and references therein), and induction was iterated to full convergence.

Comparisons of the calculated RDFs are made with experimental results (Hura *et al.* 2000; Soper 2000) and recently published results from SAPT5s+NB (Mas *et al.* 2003*a*,*b*). Results for the internal energy of the simulations are also shown.

(ii) *Results*

The oxygen RDF computed from VRT(ASP-W)III, shown in figure 3, agrees remarkably well with experiment (Hura *et al.* 2000; Soper 2000). The position of the first peak coincides almost exactly with the experimental result, particularly in comparison with neutron diffraction results (Soper 2000). More importantly, the $g(R_{\mathrm{OO}})$ predicts the signature tetrahedral structure of ambient liquid water. The first minimum of the RDF matches almost exactly, and the second maximum occurs at only *ca.* 0.15 Å from the experimental peak. VRT(ASP-W)III does yield a third solvation shell that appears to be contracted relative to experiment. However, the integral of $g(R_{\mathrm{OO}})$ from the IPS matches those from the experiments very closely, indicating that the number of nearest neighbours in the liquid is correctly described. The $g(R_{\mathrm{OH}})$ and $g(R_{\mathrm{HH}})$ from VRT(ASP-W)III agree reasonably well with the experimental results (Soper 2000). The IPS produces a liquid-phase hydrogen-bond length that is *ca.* 1.9 Å, which is very close to the experimental value.

A comparison of results from VRT(ASP-W)III with those from CPMD is shown in figure 4. The comparisons are a little more difficult to make, due to the high degree of variability of the CPMD results. All of the CPMD results were obtained using the Becke–Lee–Wang–Parr (BLYP) functional, but with varying values for the fictitious electron mass and plane-wave Rydberg cut-off. The results from VRT(ASP-W)III for $g(R_{\mathrm{OO}})$ agree best with the results from Silvestrelli & Parrinello (1999). However, as described by Grossman *et al.* (2004), the use of a high fictitious electron mass in those simulations makes their results somewhat questionable. Conversely, Grossman *et al.* (2004) use a smaller fictitious electron mass (340 versus 900 atomic units) and smaller system size (32 versus 64 $H_2O$) and obtain a $g(R_{\mathrm{OO}})$ that is much more structured than that from either Silvestrelli & Parrinello (1999) or VRT(ASP-W)III.

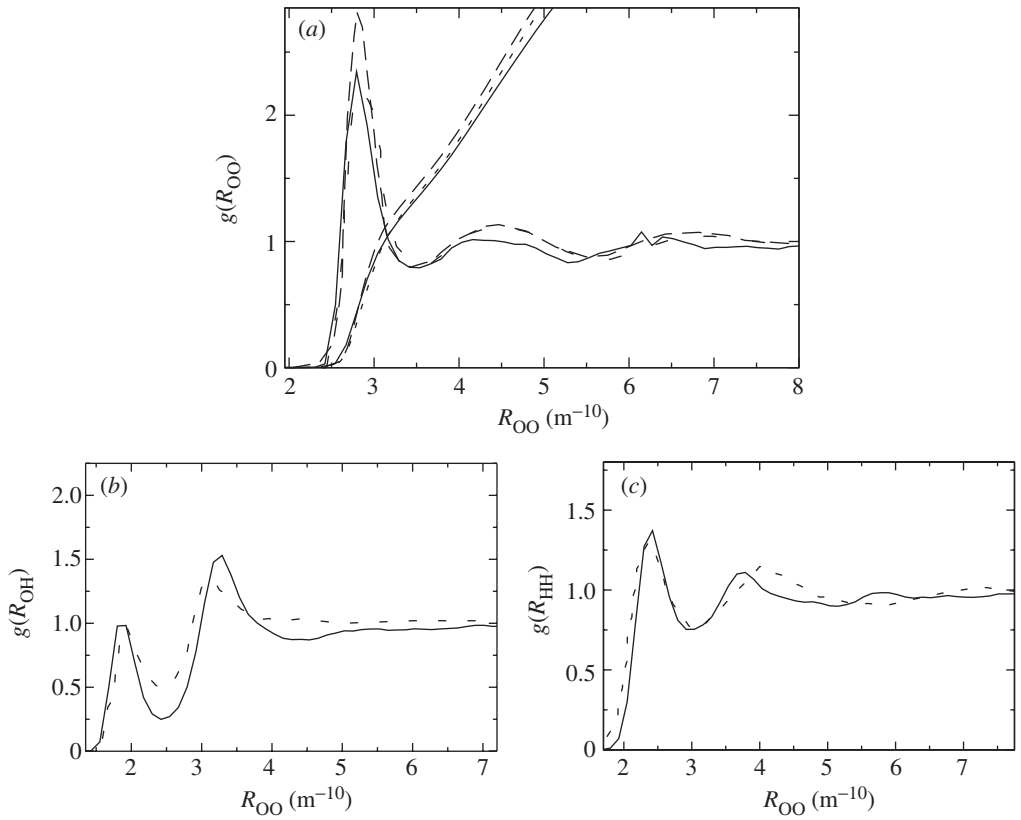


Figure 3. (*a*) $g(R_{OO})$, (*b*) $g(R_{OH})$ and (*c*) $g(R_{HH})$, for VRT(ASP-W)III, in comparison with experiment (Hura *et al.* 2000; Soper 2000). The solid curves corresponds to VRT(ASP-W)III, the dotted curves to Soper (2000) and the dashed curve to Hura *et al.* (2000). Superimposed upon the $g(R_{OO})$ plot are the respective cumulative integrals of the RDFs. Simulations were conducted in the canonical (NVT) ensemble with 64 monomers in a cubic box at ambient density of 1.0 g cm$^{-3}$ and a temperature of 25 °C. In order to extend the RDF to the end of the simulation box, the molecular configurations were duplicated in all directions, resulting in 512 configurations per time-step, when calculating this property.

In order to clarify this issue, we have performed CPMD simulations of 54 $H_2O$ with a small fictitious electron mass of 400 atomic units. The RDFs of these new CPMD simulations lie somewhere between the results of Silvestrelli & Parrinello (1999) and those of Grossman *et al.* (2004), when comparing peak heights and minima. This shows that system size effects can be nearly as large as those from choice of the fictitious electron mass. Regardless, all three RDFs from VRT(ASP-W)III compare exceedingly well with these newer CPMD results, although the comparison is not as close as to the results from Silvestrelli & Parrinello (1999). However, it is quite possible that these differences would be mitigated through experimentation with different exchange-correlation functionals and pseudopotentials.

The average potential energy of the ensemble was calculated with VRT(ASP-W)III during the course of our simulations, and the results for 298 K are shown in table 4. The experimental quantity was determined in the standard fashion, by assuming that the water vapour behaves as an ideal gas, subtracting $RT$ from the measured

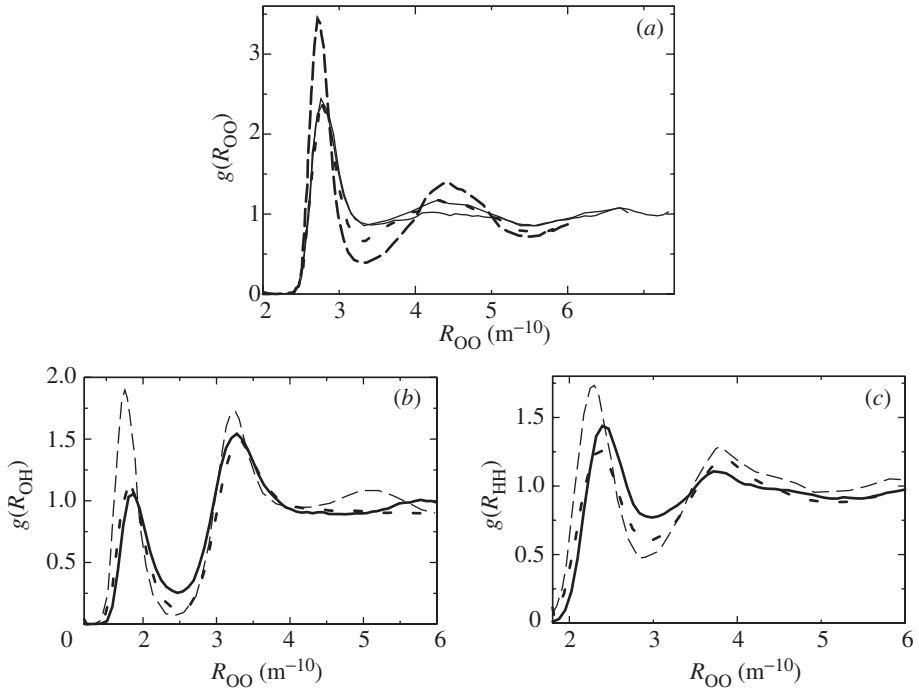


Figure 4. (*a*) $g(R_{OO})$, (*b*) $g(R_{OH})$ and (*c*) $g(R_{HH})$, for ambient water, from VRT(ASP-W)III and in comparison with results from CPMD (Grossman *et al.* 2004; Silvestrelli & Parrinello 1999). The thick solid lines correspond to VRT(ASP-W)III, the thin $g(R_{OO})$ line to Silvestrelli & Parrinello (1999), the dashed lines to Grossman *et al.* (2004), and the dotted lines to our own CPMD simulations. It is important to note that the results from Silvestrelli & Parrinello (1999) have a simulation size of 64 $H_2O$, but use an exceedingly high fictitious electron mass of 900 atomic units and a low Rydberg cut-off of 70. In contrast, the results from Grossman *et al.* (2004) use a fictitious mass of only 340 atomic units, but have an exceedingly small system size of 32 $H_2O$, and a moderate energetic cut-off of 85 Ry. Our CPMD results have a simulation size of 54 $H_2O$ and use a fictitious electron mass of 400 atomic units and an energetic cut-off of 85 Ry.

Table 4. $\Delta E_{int}$ *at* 298 K*, in comparison with the experimental value from Dorsey (1968)*

(The results from SAPT5s+NB are closer to the experimental value, but the IPS is unable to predict a tetrahedral structure in simulations of ambient liquid water (Mas *et al.* 2003*b*). TTM2-R is able to predict a reasonable liquid water tetrahedral structure, but predicts a value of $\langle E_{pot}\rangle$ that is even further from the experimental value than SAPT5s+NB (Burnham & Xantheas 2002*b*). In addition, it is important to note that TTM2-R does not have the spectroscopic accuracy of VRT(ASP-W)III.)

| | VRT(ASP-W)III | SAPT5s+NB | TTM2-R | expt |
|---|---|---|---|---|
| $\langle E_{pot}\rangle$ (kJ mol$^{-1}$) | −51.46 | −45.02 | −46.90 | −41.51 |

vaporization enthalpy at 298 K (Dorsey 1968), and multiplying the result by −1. This is equal to the value for the change in internal energy of vaporization ($\Delta E_{int}$), equal to the kinetic plus potential energy of the system. However, because we have

assumed the vapour to be an ideal gas (hence, the particles do not interact) and that the temperature of the liquid and vapour are the same (i.e. no change in kinetic energy), $\Delta E_{\mathrm{int}} = \langle E_{\mathrm{pot}} \rangle$ of the liquid. As is shown in the table, the value of $\Delta E_{\mathrm{int}}$ from VRT(ASP-W)III is within 20% of the experimental value, whereas that for SAPT5s+NB deviates from experiment by less than 9%, in the opposite direction. Thus the result from SAPT5s+NB is closer to the experimental value, but the IPS is unable to predict a tetrahedral structure in simulations of ambient liquid water (Mas *et al.* 2003*b*). TTM2-R is able to predict a reasonable liquid water tetrahedral structure, but predicts a value of $\langle E_{\mathrm{pot}} \rangle$ that is even further from the experimental value than SAPT5s+NB (Burnham & Xantheas 2002*b*). In addition, it is important to note again that TTM2-R does not have the spectroscopic accuracy of VRT(ASP-W)III.

### (*b*) *The VRT(MCY) potentials*

Recently, Leforestier *et al.* (2002) modified the original Clementi MCY potential by adding a fifth site: a floating uncharged virtual site along the $C_{2\mathrm{v}}$-axis, which is then used in place of the oxygen atom in the dispersion terms of the potential. This rigid monomer modified MCY potential was then fitted to $(H_2O)_2$ data, and shown to reproduce experimentally determined ground-state properties and excited intermolecular vibrational state band origins very well. The resulting IPS was named VRT(MCY-5r), where the 'VRT' corresponds to the vibration–rotational–tunnelling data to which it was fitted, and '5r' corresponds to the five sites of the rigid monomer potential.

In an effort to include many-body interactions in the above potential, a functional form developed by Bernardo *et al.* (1994), containing *ab initio* atomic polarizabilities, was added to model the many-body induction energy (Leforestier *et al.* 2005). This new potential was named VRT(MCY-5r/pol), where 'pol' refers to the fact that the water monomers have polarizable sites. While this IPS is also able to reproduce experimental observables of the water dimer to a high degree of accuracy (Leforestier *et al.* 2005), DMC calculations performed by us show that both of the above potentials yield inaccurate ground-state structural properties for $(H_2O)_2$. For example, both of the above IPSs yield vibrational ground-state average O–O distances between the monomers, $\langle R_{\mathrm{OO}} \rangle$, which are between 3.10 and 3.20 Å, compared with the experimental value of 2.99 Å (Dyke *et al.* 1977). Hence, in terms of modelling clusters larger than the dimer or of modelling the liquid, this IPS does not have a sufficient level of accuracy. However, VRT(MCY-5r/pol) is included in the present discussion because of its relatively simple functional form, and since it provides helpful comparison with results from the SAPT5s+NB IPS.

#### (i) *Molecular dynamics simulations*

Due to its simplicity, VRT(MCY-5r/pol) could be simulated via MD. This had the advantage of allowing us to determine dynamical as well as structural information about the potential. Due to the fact that the IPS has electrostatic terms no larger than the dipole, it was possible to use full Ewald sums in the simulations. The minimum image convention was applied when calculating distances between centre of masses of molecules, and all short-range interactions were truncated within a cut-off radius equal to half the box length. Our simulations were conducted in the

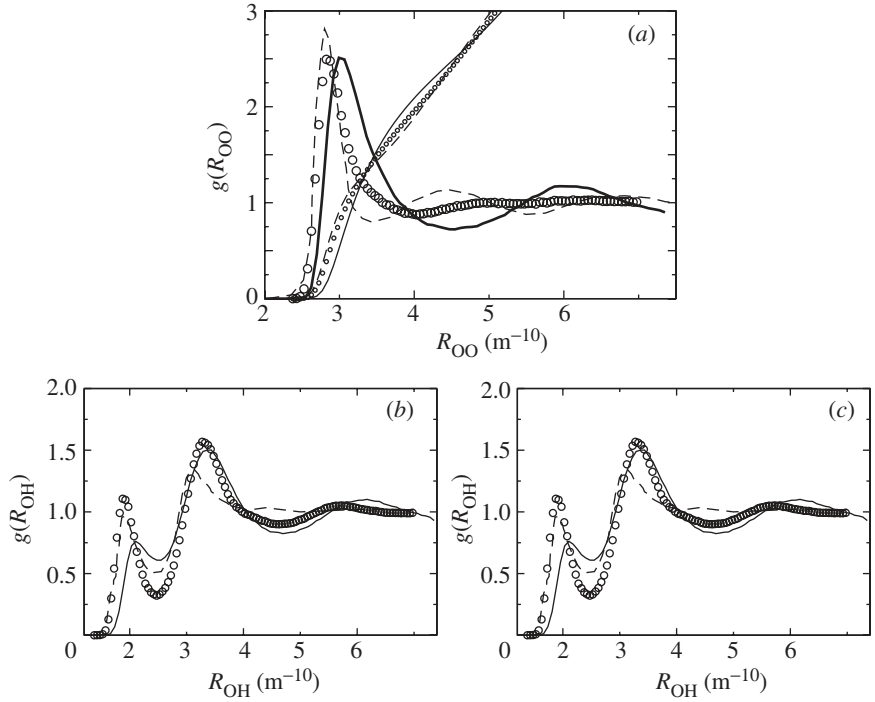


Figure 5. (*a*) $g(R_{OO})$, (*b*) $g(R_{OH})$ and (*c*) $g(R_{HH})$, for VRT(MCY-5r/pol), in comparison with SAPT5s+NB (Mas *et al.* 2003*b*) and experiment (Hura *et al.* 2000). The solid curves correspond to VRT(MCY-5r/pol), the open circles to Mas *et al.* (2003*b*) and the dashed curve to Hura *et al.* (2000). Again, superimposed upon the $g(R_{OO})$ plot are the respective cumulative integrals of the RDFs. Simulations were conducted in the canonical (NVT) ensemble with 108 monomers in a cubic box at ambient density of 1.0 g cm$^{-3}$ and a temperature of 25 °C.

canonical (NVT) ensemble with 32–256 monomers in a cubic box at an ambient density of 1.0 g cm$^{-3}$ and a temperature of 25 °C.

This section describes our MD simulation results from VRT(MCY-5r/pol). The liquid structure was found to saturate at simulation sizes of 108 monomers, and results from 256-monomer simulations are presented herein. A time-step of 0.5 fs was used for the intermolecular force field for both IPSs, and all simulations were run for a total of 10 ps.

(ii) *Results*

The RDFs for VRT(MCY-5r/pol) are shown in figure 5, with comparison made with results from SAPT5s+NB (Mas *et al.* 2003*b*) and experiment (Hura *et al.* 2000; Soper 2000). For VRT(MCY-5r/pol), the first peak of the $g(R_{OO})$ occurs at too large a distance (*ca.* 10%), which is to be expected considering the overestimation of the dimer vibrational ground-state $\langle R_{OO} \rangle$ by the IPS. Nonetheless, for $g(R_{OO})$, the result does not exhibit the requisite second (tetrahedral) peak at *ca.* 4.5 Å, and interestingly resembles the RDF of a Lennard-Jones fluid. In addition, there exists a clearly visible but small third solvation shell at *ca.* 9 Å (not shown for the sake of clarity). The $g(R_{OH})$ has too small a first peak (*ca.* 20% too low) and predicts

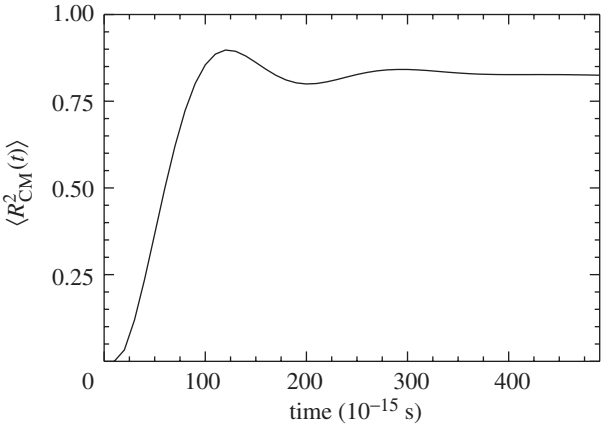


Figure 6. $\langle R^2_{CM}(t)\rangle$ for VRT(MCY-5r/pol) (solid line) at 298 K.
The slope of the curve at $t \gg 0$ yields the value of the diffusion constant, $D$.

a hydrogen-bond length of 2 Å. However, the second peak matches reasonably well with experiment. Finally, the shape of the $g(R_{HH})$ matches the experimental results well, although the two peaks are slightly too close together, as was the case for VRT(ASP-W)III. Also, both $g(R_{OH})$ and $g(R_{HH})$ of VRT(MCY-5r/pol) exhibit the third solvation shell at *ca.* 6 Å.

The fact that these results are very similar to those from SAPT5s+NB is also interesting. The maximum of the first peak from SAPT5s+NB is closer to the experimental value, but it is similarly too wide and the $g(R_{OO})$ also lacks the second maximum at 4.5 Å. Thus, this behaviour appears to be a general characteristic of 'spectroscopic' potentials with functional forms simpler than that of ASP-W, used to model the liquid. Interestingly, integration of the plots of $g(R_{OO})$ in figure 5 shows that the RDFs from both VRT(MCY-5r/pol) and SAPT5s+NB yield cumulative sums that are strikingly similar to that of the experimental curve. This implies that all three results yield roughly the same number of nearest neighbours, when comparing the values of the integral up to the first minimum, despite the fact that VRT(MCY-5r/pol) and SAPT5s+NB do not yield tetrahedral liquid structure.

The IPS was further assessed through calculation of the mean squared displacement of the centre of mass of each monomer, $\langle R^2_{CM}(t)\rangle$. From this, the diffusion constant ($D$) can be determined by calculating the slope of the curve in figure 6. The plot shows yet another remarkable feature: the potential yields a diffusion constant of zero (for the time-scale of our simulation). In order to get the monomers simulated on the VRT(MCY-5r/pol) surface to diffuse on the time-scales of our calculations, these simulations were run at temperatures as high as 598 K, yet no significant change was found in the $\langle R^2_{CM}(t)\rangle$ curve or the RDFs.

## 5. Discussion

VRT(ASP-W)III, the recently developed polarizable, six-dimensional water dimer potential, has been tested in simulations of liquid water at ambient conditions. We have shown that this spectroscopic 'first principles' polarizable dimer potential reproduces the vibrational ground-state structures of the trimer through hexamer as well as the detailed vibration–rotational–tunnelling states of the dimer, and thus is a

good start toward developing a 'universal potential' for water. VRT(ASP-W)III is able to produce a $g(R_{\mathrm{OO}})$ reflecting the tetrahedral structure characteristic of liquid water. The $g(R_{\mathrm{OH}})$ and $g(R_{\mathrm{HH}})$ calculated from the IPS also compare favourably with experiments (Soper 2000) in terms of peak positions but, for $g(R_{\mathrm{OH}})$, the first peak is still too low and the second peak too high; for $g(R_{\mathrm{HH}})$ the peaks are too close together. Interestingly, the results from two other spectroscopic surfaces, VRT(MCY-5r/pol) and SAPT5s+NB, do not predict tetrahedral liquid water structure, and yet both IPS predict $g(R_{\mathrm{OH}})$ and $g(R_{\mathrm{HH}})$ functions that compare favourably with experiments. It should be noted again that simulations with all three rigid, 'spectroscopic' potentials exhibit a number of nearest neighbours within the first solvation shell that agrees very well with experiment (within *ca.* 5%), despite the fact that the much simpler SAPT5s+NB and VRT(MCY-5r) IPSs yield inaccurate liquid structures. The most striking differences between VRT(ASP-W)III and the previous two IPSs is that this third fitting of ASP-W was fitted to a much larger set of experimental data. This gives clear testament to the fact that exact determination of the water dimer IPS is a very subtle process, wherein small changes in the potential can have large ramifications for the predicted properties of condensed phases.

It is interesting to note once again that Burnham & Xantheas (2002*b*) were able to achieve some level of 'universality' in their TTM2-R potential, by fitting a 6-10-12 Lennard-Jones functional form to only 25 very-high-level *ab initio* points calculated along the $C_{\mathrm{s}}$ symmetry. While the potential is highly accurate for geometries within that symmetry, it does not have the same level of accuracy for the energetics of others (namely $C_2$, $C_{\mathrm{i}}$, and $C_{2\mathrm{v}}$) and, as we note above, is not an accurate model for the dimer VRT spectrum. However, it does yield good results for those bulk properties tested by Burnham & Xantheas (2002*b*). Hence, it would be very interesting to refine their potential via comparison with experimental data, to see what effect (positive or negative) this would have on the accuracy of its structural predictions for liquid water and ice. In addition, Burnham & Xantheas (2002*c*) have developed the TTM2-F potential, which includes both *intra*molecular flexibility and a monomer-geometry-dependent polarization. TTM2-F yields highly accurate water- cluster-equilibrium, non-quantum-corrected energetics and accurately describes monomer geometry deformation with increasing cluster size, and thus appears to achieve a higher level of 'universality' than its predecessor, TTM2-R. Consequently, it would be interesting to investigate its predictive powers in terms of the dimer VRT spectrum and larger cluster vibrational ground states.

The value $\Delta E_{\mathrm{int}}$ yielded from VRT(ASP-W)III is too low, and could easily be due to the exclusion of nuclear quantum effects in our simulations. Treatment of quantum effects in liquid simulations is beyond the scope of this paper, and the reader is referred to Feynman & Hibbs (1965), Schulman (1981) and Feynman (1998) for discussions. Nonetheless, quantum effects in liquid water are generally regarded as being fairly small, and a rule of thumb is that they are equivalent to raising the temperature of a simulation by 50 °C (Del Buono *et al.* 1991; Kuharsky & Rossky 1985). However, it is quite possible that the quantum effects in the liquid will be far more dramatic when using a spectroscopic potential, such as VRT(ASP-W)III, that is derived from an explicitly quantum dynamical model. In an empirical liquid-water potential, a classical simulation is used to fit the potential to experimental results. Consequently, any potential energy barrier between configurations will be artificially flattened in order to effectively allow classical mechanics to represent tunnelling

effects and zero-point effects. As a result, it is not surprising that such potentials exhibit small apparent quantum effects. However, a 'spectroscopic' potential, formulated from first principles, will not exhibit the same artificial lowering of tunnelling barriers. Hence, tunnelling effects in the liquid could be significant, as could familiar zero-point effects. This should be explored in future work.

This work was supported by the Experimental Physical Chemistry Program of the National Science Foundation (NSF). The authors thank Larry Fried of Lawrence Livermore National Laboratory for many helpful discussions. R.J.S. and C.F. gratefully acknowledge a grant from the Integrated Programs Division of the NSF.

## References

Allen, M. P. & Tildesley, D. J. 1989 *Computer simulations of liquids*. Oxford: Clarendon.

Berendsen, H. J. C., Grigera, J. R. & Straatsma, T. P. 1987 *J. Phys. Chem.* **91**, 6269.

Bernardo, D. N., Ding, Y., Krogh-Jespersen, K. & Levy, R. M. 1994 *J. Phys. Chem.* **98**, 4180.

Braly, L. B. 1999 PhD thesis, University of California, Berkeley, CA, USA.

Braly, L. B., Cruzan, J. D., Liu, K., Fellers, R. S. & Saykally, R. J. 2000*a* *J. Chem. Phys.* **112**, 10 293.

Braly, L. B., Liu, K., Brown, M. G., Keutsch, F. N., Fellers, R. S. & Saykally, R. J. 2000*b* *J. Chem. Phys.* **112**, 10 314.

Buch, V. 1992 *J. Chem. Phys.* **97**, 726.

Burnham, C. J. & Xantheas, S. 2002*a* *J. Chem. Phys.* **116**, 1479.

Burnham, C. J. & Xantheas, S. 2002*b* *J. Chem. Phys.* **116**, 1500.

Burnham, C. J. & Xantheas, S. 2002*c* *J. Chem. Phys.* **116**, 5115.

Busarow, K. L., Cohen, R. C., Blake, G. A., Laughlin, K. B., Lee, Y. T. & Saykally, R. J. 1989 *J. Chem. Phys.* **90**, 3937.

Del Buono, G. S., Rossky, P. J. & Schnitker, J. 1991 *J. Chem. Phys.* **95**, 3728.

Dorsey, N. E. 1968 *Properties of ordinary water: substance*. New York: Hafner.

Dyke, T. R., Mack, K. M. & Muenter, J. S. 1977 *J. Chem. Phys.* **66**, 498.

Fellers, R. S., Leforestier, C., Braly, L., Brown, M. G. & Saykally, R. J. 1999 *Science* **284**, 945.

Feynman, R. P. 1998 *Staistical mechanics*. Reading, MA: Addison-Wesley.

Feynman, R. P. & Hibbs, A. R. 1965 *Quantum mechanics and path integrals* New York: McGraw-Hill.

Frenkel, D. & Smit, B. 1996 *Understanding molecular simulation* San Diego: Academic.

Goldman, N. & Saykally, R. J. 2004 *J. Chem. Phys.* **120**, 4777.

Goldman, N., Fellers, R. S., Brown, M. G., Braly, L. B., Keoshian, C. J., Leforestier, C. & Saykally, R. J. 2002 *J. Chem. Phys.* **116**, 10 148.

Gregory, J. K. & Clary, D. C. 1994 *Chem. Phys. Lett.* **228**, 547.

Gregory, J. K. & Clary, D. C. 1995*a* *J. Chem. Phys.* **102**, 7817.

Gregory, J. K. & Clary, D. C. 1995*b* *J. Chem. Phys.* **103**, 8924.

Gregory, J. K. & Clary, D. C. 1996*a* *J. Phys. Chem.* **100**, 18014.

Gregory, J. K. & Clary, D. C. 1996*b* *J. Chem. Phys.* **105**, 6626.

Gregory, J. K., Clary, D. C., Liu, K., Brown, M. G. & Saykally, R. J. 1997 *Science* **275**, 814.

Groenenboom, G. C., Mas, E., Bukowski, R., Szalewicz, K., Wormer, P. E. S. & van der Avoird, A. 2000 *Phys. Rev. Lett.* **84**, 4072.

Grossman, J., Schwegler, E., Draeger, E. W., Gygi, F. & Galli, G. 2004 *J. Chem. Phys.* **120**, 300.

Guillot, B. 2003 *J. Mol. Liquids* **101**, 219.

Hodges, M. P., Stone, A. J. & Xantheas, S. S. 1997 *J. Phys. Chem. A.* **101**, 9163.

Hura, G., Sorenson, J. M., Glaser, R. M. & Head-Gordon, T. 2000 *J. Chem. Phys.* **113**, 9140.

Jorgensen, W. L., Chandrasekhar, J., Madura, J. D., Impey, R. W. & Klein, M. L. 1983 *J. Chem. Phys.* **79**, 926.

Kell, G. S., McLaurin, G. E. & Whalley, E. 1989 *Proc. R. Soc. Lond. A* **425**, 49.

Keutsch, F. N. & Saykally, R. J. 2001 *Proc. Natl Acad. Sci. USA* **98**, 10 533.

Kloppera, W., Quack, M. & Suhm, M. A. 1998 *J. Chem. Phys.* **108**, 10096.

Kuharsky, R. A. & Rossky, P. J. 1985 *J. Chem. Phys.* **82**, 5164.

Leforestier, C., Gatti, F., Fellers, R. S. & Saykally, R. J. 2002 *J. Chem. Phys.* **117**, 8710.

Leforestier, C., Goldman, N. & Saykally, R. J. 2005 (In preparation.)

Liu, K., Loeser, J. G., Elrod, M. J., Host, B. C., Rzepiela, J. A. & Saykally, R. J. 1994 *J. Am. Chem. Soc.* **116**, 3507.

Liu, K., Cruzan, J. D. & Saykally, R. J. 1996*a* *Science* **271**, 929.

Liu, K., Brown, M. G., Carter, C., Saykally, R. J., Gregory, J. K. & Clary, D. C. 1996*b* *Nature* **381**, 501.

Liu, K., Brown, M. G., Cruzan, J. D. & Saykally, R. J. 1996*c* *Science* **271**, 62.

Liu, K., Brown, M. G. & Saykally, R. J. 1997 *J. Phys. Chem. A* **101**, 8995.

McGlashan, M. L. & Wormald, C. J. 2000 *J. Chem. Thermo.* **32**, 1489.

Mas, E. M., Bukowski, R. & Szalewicz, K. 2003*a* *J. Chem. Phys.* **118**, 4386.

Mas, E. M., Bukowski, R. & Szalewicz, K. 2003*b* *J. Chem. Phys.* **118**, 4404.

Matsuoka, O., Clementi, E. & Yoshimine, M. 1976 CI study of the water dimer potential surface. *J. Chem. Phys.* **64**, 1351–1361.

Millot, C. & Stone, A. J. 1992 *Mol. Phys.* **77**, 439.

Ojamäe, L. & Hermansson, K. 1994 *J. Phys. Chem.* **98**, 4271.

Pugliano, N. & Saykally, R. J. 1992 *Science* **257**, 1937.

Quack, M. & Suhm, M. A. 1990 *Mol. Phys.* **69**, 79.

Quack, M. & Suhm, M. A. 1991*a* *Chem. Phys. Lett.* **183**, 187.

Quack, M. & Suhm, M. A. 1991*b* *J. Chem. Phys.* **95**, 28.

Quack, M., Stohner, R. & Suhm, M. A. 2001 *J. Mol. Struct.* **599**, 381.

Rybak, S., Jeziorski, B. & Szalewicz, K. 1991 *J. Chem. Phys.* **95**, 6576.

Ryckaert, J.-P., Ciccotti, G. & Berendsen, H. J. C. 1977 *J. Computat. Phys.* **23**, 327.

Sandler, P., Jung, J. O., Szczesniak, M. M. & Buch, V. 1994 *J. Chem. Phys.* **101**, 1378.

Saykally, R. J. & Blake, G. A. 1993 *Science* **259**, 1570.

Schulman, L. S. 1981 *Techniques and applications of path integration*. Wiley.

Silvestrelli, P. L. & Parrinello, M. 1999 *Phys. Rev. Lett.* **82**, 3308.

Soper, A. K. 2000 *Chem. Phys.* **258**, 121.

Stone, A. J. 1996 *The theory of intermolecular forces*. International Series of Monographs on Chemistry, vol. 32. Oxford: Clarendon.

Stone, A. J., Dullweber, A., Engkvist, O., Fraschini, E., Hodges, M. P., Meredith, A. W., Popelier, P. L. A. & Wales, D. J. 2000 ORIENT*: a program for studying interactions between molecules*, v. 4.4, University of Cambridge. (Available at http://fandango.ch.cam.ac.uk/.)

Xantheas, S., Burnham, C. J. & Harrison, R. J. 2002 *J. Chem. Phys.* **116**, 1493.